Journal of Solid Mechanics Vol. 17, No. 2 (2025) pp. 183-196
DOI: 10.60664/jsm.2025.1189055

Research Paper

Fluid-Solid-Interaction in Radial Vibration of Carbon Nanotubes Immersing in Compressible Fluid

A. Fatahi-Vajari [1*], Z. Azimzadeh [2]

[1] *Department of Mechanical Engineering, Shahriar Branch, Islamic Azad University, Shahriar, Iran*
[2] *Department of Mathematics, College of Basic Sciences, Yadegar-e-Imam Khomeini (RAH)Shahre Rey Branch, Islamic Azad University, Tehran, Iran*

Received 11 November 2024; Received in revised form 3 March 2025; Accepted 6 March 2025

ABSTRACT

This paper investigates the radial breathing mode (RBM) vibration of single-walled carbon nanotubes (SWCNTs) in a fluid media. Doublet mechanics (DM) model is used to consider microstructural features of the tube along with Navier-stoke's equation is considered to incorporate fluid properties. The medium surrounding the nanotube is typically modeled as a compressible Newtonian fluid and purely radial vibration of an elastic nanotube called the breathing mode in fluid is studied. An implicit partial differential equation that governs the RBM vibration of SWCNTs vibrating in fluid is derived and then solved using fluid-solid intraction in boundaries to give the damped frequency of the tube. Because of fluid interaction with the nanotube, the frequency obtained has complex form which in real part is the main frequency and the imaginary part represents the damping severity. The effects of microstructure along with fluid compressibility and viscosity in the breathing mode of an elastic nanotube are discussed in details. The results obtained herein are compared with the existing theoretical and experimental results and good agreement especially with the latter is observed.

Keywords: Doublet mechanics; Damped frequency; Fluid-solid interaction; Single-walled carbon nanotubes; Radial vibration; Compressible Newtonian fluid.

1 INTRODUCTION

CARBON nanotubes (CNTs) are perfect tiny and hollow cylinder with unique electromechanical behaviors. They have attracted worldwide attention for their potential use as nano-pipes conveying fluids [1, 2]. For example, researchers have found that CNTs could be filled with liquid metal to become the smallest thermometers

*Corresponding author. Tel.: +98 9125365747.
E-mail address: afatahiv@iau.ac.ir (A. Fatahi-Vajari)

[3]. In addition, biological nanoparticles such as viruses have also been modeled as elastic spheres in the studies of their vibration characteristics in different media with ultrasound waves via resonance [4]. Nanopipes that behave as tiny straws could deliver medicines, very slowly to a person's bloodstream or to a highly specific location in the body [5]. Studies on the vibration of elastic nanoparticles embedded in fluid media have recently attracted considerable interest, because of potential applications, for example, as an alternative nondestructive instrument for determining the properties of the material and designing mechanical and biological sensors [6]. The resonant frequencies and damping characteristics of mechanical nanostructures with different shapes have been measured by a variety of experimental methods [7]. Because of unique transport properties of CNTs for conveying fluid, investigating the physical and mechanical properties of fluid-filled CNTs is essential and their applications in nanoengineering are a controversial research topic [8, 9]. In addition, interest in fluid-filled SWCNTs is rising due to the progress in large-scale synthesis of them. Based on these considerations, it is very significant to study the vibration characteristics of fluid-filled CNTs. Low damping and high quality factor are desirable in these applications for detecting with high sensitivity. Therefore, studying of damping mechanisms is of much concern due to energy dissipation or energy transfer to the surrounding media. Ruijgrok and et al. combined ultrafast pump–probe spectroscopy with optical trapping to investigate homogeneous damping of the acoustic vibrations of nanospheres and nanorods in water [10]. From the modeling point of view, acoustic vibrations of elastic bodies are classical problems in CCM. For example, Fatahi-Vajari and Imam [11-13] studied theoretically the vibrations of an elastic tube in vacuum with different geometries. The effect of chirality in nanotubes was investigated by Ebrahimian et al. [14-16]. Ebrahimian et al. studied the nonlinear buckling behavior of a composite rectangular plate reinforced with graphene nanosheets, employing the third-order shear deformation principle [17]. In addition, the effect of different surrounding environments, including an elastic solid matrix and inviscid and viscous fluid media, were also considered in later studies [18]. As a remark, for a nanoparticle with a typical size of tens of nanometers, the atomic spacing is usually sufficiently small that a CCM description is valid. Such an approach was also shown to be successful in predicting the resonant frequency (on the order of tens of GHz) of a gold nanoparticle vibrating in water [19, 20]. Recently, an experiment on the vibration of a bi-pyramidal gold nanoparticle in water-glycerol mixtures suggested that the high frequency vibration could trigger viscoelastic responses in the mixture [21, 22].

The continuum models have been widely used to discuss the mechanical behaviors of fluid-filled MWCNTs. For example, Yan et al. [23] exhibited the dynamical stability behaviors of fluid-conveyed MWCNTs and determined the critical flow velocities associated with divergence, restabilization and utter. Natsuki et al. [24] presented sound wave propagation in both SWCNTs and DWCNTs filled with fluid and found that the wave propagation in fluid-filled CNTs was affected largely by the speed of free wave in the fluid. Dong et al. [25] reported the results of an investigation into the wave dispersion characteristic in fluid-filled CNTs embedded in an elastic medium and described the effects of shear deformation, rotary inertia and elastic matrix on the velocity, critical frequency, cut-of frequency and amplitude ratio of wave propagation in MWCNTs. Experiments on the acoustic vibrations of elastic nanostructures in Newtonian fluid media have been used to study the mechanical properties of materials [9]. Ghobanpour Arani et al. proposed a nonlocal foundation model to analyze the vibration and instability of a Y-shaped Y-SWCNT conveying fluid using Eringen's nonlocal theory [26]. Rexy et al. studied the nonlocal elastic waves in a fluid conveying Armchair thermoelastic SWCNT under moving harmonic load using Eringen's nonlocal elasticity theory via Euler Bernoulli beam equation [27]. Coupled vibration of nanotube has been studied in many papers like [28, 29]. On the other hands, one of the most important applications of vibrating nanotubes in fluid is in fabrication of nanosensors acting in fluid media [30, 31].

Four distinct categories of materials that have attracted significant attention are nanomaterials, macromaterials, micromaterials, and smart materials. These categories span a wide spectrum of size, structure, and functionality, effecting their applications across various industries. Nanomaterials operate at the nanoscale, exhibiting exceptional properties due to their small size. Macromaterials encompass large-scale structures and materials often seen in everyday life. Micromaterials, on the other hand, bridge the gap between nano and macro by focusing on materials at the microscale. Finally, smart materials are designed to respond dynamically to external stimuli, offering unique adaptability and versatility.

The following table lists the differences between nano, macro, micro and smart materials.

Table 1
Comparison between different main categories of materials

Property	Nano Material	Macro Material	Micro Material	Smart Material
Size	Dimensions lesser than 100 nanometers (nm).	Dimensions larger than 1 millimeter (mm).	Dimensions about 5 micrometers (μm).	Varies, not defined by size.
Examples	Carbon nanotubes, nanoparticles.	Metals, plastics, ceramics.	MEMS devices, microelectronics.	Shape-memory alloys, piezoelectric materials.
Behavior	Unique properties due to small size.	Common properties at visible scale.	Intermediate properties and behavior.	Respond to external stimuli.
Observability	Requires specialized tools like microscopes.	Visible to the naked eye.	Requires specialized tools like microscopes.	Observable through functionality.
Applications	Nanomedicine, nanoelectronics.	Construction, manufacturing.	MEMS devices, microsensors.	Sensors, actuators, adaptive systems.
Size-related	Size-dependent properties.	Bulk properties.	Intermediate scale.	Not size-dependent, functionality-based.

It should be pointed out that the RBM is the characteristic phonon mode of SWCNTs which leads to a periodic increase and decrease of the tube diameter. This feature is specific to CNTs and is not observed in other carbon systems such as graphite [13]. On the other hand, this frequency is usually the strongest feature in SWCNT Raman spectra which plays a crucial role in the experimental determination of the geometrical properties of SWCNTs [32]. Furthermore, studying radial vibration of nanotubes conveying fluid is very significant for manufacturing and production nanosensors. Therefore, it is very important to know the behavior of RBM frequency of different nanotubes, precisely.

Although the vibration of fluid-conveying nanotube has been studied more but to the Authors best knowledge, studies on RBM vibration characteristics in SWCNTs which are immersed in fluid are not particularly investigated in the literature yet and the present paper attempts to consider such problem. In this paper, first the classical problem of the breathing mode of a vibrating elastic tube in a vacuum is revisited and then is extend to complex fluid media. When interactions between the tube and fluid need to be considered, the vibration frequency is significantly different from the empty one. Therefore, we focus on the dynamical behaviors of a fluid-filled SWCNT with considering scale effect by using DM model. The paper has been organized by first presenting a DM formulation in Section 1.2 for the elasticity problem of a radially vibrating nanotube and in section 2.2 the propagation of acoustic waves in the fluid medium. The two problems are then coupled by matching the velocities and stresses at the interface of the solid in section 3. An analytical eigenvalue equation determining the vibration frequencies of an elastic nanotube in a compressible, viscous, Newtonian fluid medium is also obtained in this section. The results are validated against previous theoretical and experimental studies of a vibrating nanotube. The calculations are then extended and studied in detail in Section 4, with results and remarks discussed.

2 FORMULATION

In this section, the basic equations of motion for the nanotube are derived and the interaction between fluid and structure are investigated in the later section.

2.1 Radial vibration of nanotube

The governing equations for RBM vibration of SWCNTs are derived. Now, consider a SWCNT of length L, mean radius R, Young's modulus E, Poisson's ratio ν and mass density ρ as shown in Fig. 1. The direction in radial, polar and axial are denoted by r,θ and z, respectively. The corresponding displacements are introduced by u_r,u_θ and u_z respectively.

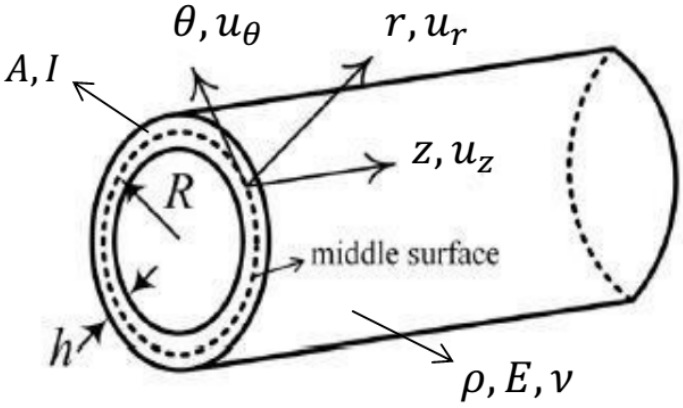

Fig. 1
A nanotube in cylindrical coordinate [34].

The basic equations of motion for a nanotube based on thin shell theory are as follow [11, 12]

$$\frac{\partial N_{zz}}{\partial z}+\frac{1}{r}\frac{\partial N_{\theta z}}{\partial \theta}+\rho f_z=\rho\frac{\partial^2 u_z}{\partial t^2} \tag{1}$$

$$\frac{\partial N_{z\theta}}{\partial z}+\frac{1}{r}\frac{\partial N_{\theta\theta}}{\partial \theta}+\frac{N_{\theta r}}{r}+\rho f_\theta=\rho\frac{\partial^2 u_\theta}{\partial t^2} \tag{2}$$

$$\frac{\partial N_{zr}}{\partial z}+\frac{1}{r}\frac{\partial N_{\theta r}}{\partial \theta}-\frac{N_{\theta\theta}}{r}+\rho f_r=\rho\frac{\partial^2 u_r}{\partial t^2} \tag{3}$$

$$\frac{\partial M_{zz}}{\partial z}+\frac{1}{r}\frac{\partial M_{\theta z}}{\partial \theta}+\rho \bar{l}_z=N_{zr} \tag{4}$$

$$\frac{\partial M_{z\theta}}{\partial z}+\frac{1}{r}\frac{\partial M_{\theta\theta}}{\partial \theta}+\frac{1}{r}M_{\theta r}+\rho \bar{l}_\theta=N_{\theta r} \tag{5}$$

$$\frac{M_{zr}}{\partial z}+\frac{1}{r}\frac{M_{\theta r}}{\partial \theta}-\frac{M_{\theta\theta}}{r}+\rho \bar{l}_r=N_{rr} \tag{6}$$

wherein f_i and $\bar{l}_\theta$ are body forces and body couples, respectively.

Also, assuming that the shell-like body is thin, the physical components N_{ij} and M_{ij} are written as:

$$N_{ij}=\int_{-\frac{h}{2}}^{\frac{h}{2}}\sigma_{ij}^{(M)}dz \ \ ,i,j=1,2,3 \tag{7}$$

$$M_{ij}=\int_{-\frac{h}{2}}^{\frac{h}{2}}z\,\sigma_{ij}^{(M)}dz \ \ ,i,j=1,2,3 \tag{8}$$

In order to overcome to the classical continuum mechanics (CCM) limitations [37], various important modifications to CCM were suggested to enter microstructural features into the theory. One of the most important generalized continuum theories that have recently been applied to materials with microstructure is doublet

mechanics (DM). This theory originally developed by Granik (1978), has been applied to granular materials by Granik and Ferrari (1993) and Ferrari et al. (1997) [35]. In DM micromechanical models, solids are represented as arrays of points, particles or nodes at finite distances. This theory has shown good promise in predicting observed behaviors that are not predictable using continuum mechanics like Flamant paradox and also dispersive wave propagation [36]. In this section, this theory is used to obtain the basic equations of motion for CNTs.

From DM principles, the microstrains with only three terms approximation can be written in cylindrical coordinates as [32]:

$$\epsilon_\alpha = \boldsymbol{\tau}^0_\alpha.\left(\boldsymbol{\tau}^0_\alpha.\nabla \boldsymbol{u}\right)+\frac{1}{2}\eta_\alpha\left[\boldsymbol{\tau}^0_\alpha.\left(\boldsymbol{\tau}^0_\alpha.\nabla\right)\left(\boldsymbol{\tau}^0_\alpha.\nabla \boldsymbol{u}\right)\right]+\frac{1}{6}\eta_\alpha^2\left[\boldsymbol{\tau}^0_\alpha.\left(\boldsymbol{\tau}^0_\alpha.\nabla\right)\left(\boldsymbol{\tau}^0_\alpha.\nabla\right)\left(\boldsymbol{\tau}^0_\alpha.\nabla \boldsymbol{u}\right)\right] \tag{9}$$

wherein $\epsilon_\alpha, \boldsymbol{\tau}^0_\alpha$ and u are microstrain, branch vector and displacement vector, respectively**.** The gradient operator ∇ in cylindrical coordinates is given by

$$\nabla = \frac{\partial}{\partial r}\boldsymbol{e}_r+\frac{1}{r}\frac{\partial}{\partial \theta}\boldsymbol{e}_\theta+\frac{\partial}{\partial z}\boldsymbol{e}_z \tag{10}$$

Similarly to Eq. (9), the macro- to microstress relations, to within three terms in the expansion, in the cylindrical coordinates may be written as [34]:

$$\boldsymbol{\sigma}^{(M)} = \sum_{\alpha=1}^{n}\boldsymbol{\tau}^0_\alpha\boldsymbol{\tau}^0_\alpha\left\{\left(p_\alpha-\frac{1}{2}\eta_\alpha\boldsymbol{\tau}^0_\alpha.\left(\nabla p_\alpha\right)+\frac{1}{6}\eta_\alpha^2\left[\left(\boldsymbol{\tau}^0_\alpha.\nabla\right)\left(\boldsymbol{\tau}^0_\alpha.\nabla p_\alpha\right)\right]\right)\right\} \tag{11}$$

In this study, the following assumptions for cylindrical shells are made. First, all points that lie on a normal to the middle surface remain the same before and after the deformation. It can be assumed that the transverse shear stresses $\sigma_{rz}^{(M)}$ and $\sigma_{\theta z}^{(M)}$ are to be negligible. Second, displacements are small compared to the shell thickness.

As is known, in the RBM, all carbon atoms move coherently in the radial direction creating a breathing-like vibration of the entire tube. Thus, with assumptions of axisymmetric and homogeneity for the entire tube in the RBM vibration, this implies that $\frac{\partial}{\partial \theta}=0, \frac{\partial}{\partial \mathrm{r}}=0$ and $u_\theta = 0$. Considering such assumptions, Eqs. (1)- (6) reduce to

$$-\frac{N_{\theta\theta}}{r}+\rho f_r = \rho\frac{\partial^2 u_r}{\partial t^2} \tag{12}$$

In the DM, the relation between microstress and microstrain in isotropic media with local interactions is given by

$$p_\alpha = A_0\epsilon_\alpha \tag{13}$$

As a result of the above assumptions, the gradient operator and the displacement vector are given by:

$$\nabla = \frac{\partial}{\partial r}\boldsymbol{e}_r, \boldsymbol{u} = u_r\left(z\right)\boldsymbol{e}_r \tag{14}$$

It is further assumed that all doublets originating from a common node have the same magnitudes, i.e., $\eta_a = \eta, a = 1,2,3$.

As mentioned above, a SWCNT is constructed from three doublets having equal lengths and angles between them, an example of which is a Zigzag SWCNT shown in Fig. 2.

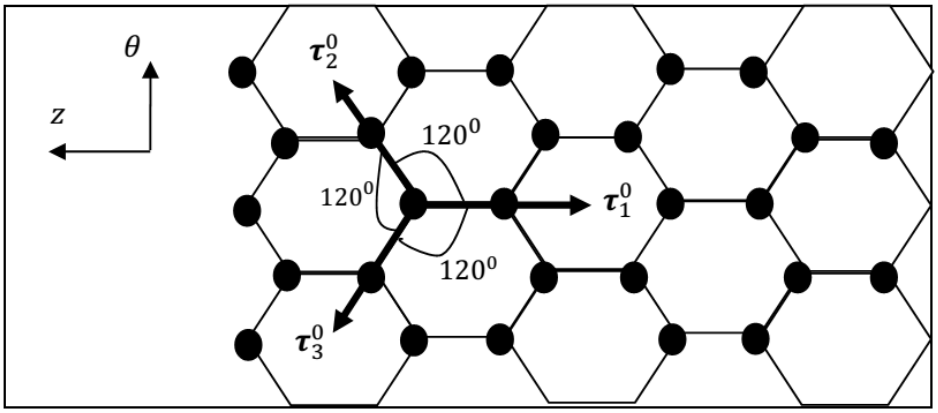

Fig. 2
A Zigzag nanotube [34].

Considering Fig. 2, the director vectors in cylindrical coordinates can be expressed as:

$$\tau_{1r}^0 = 0\ ,\tau_{2r}^0 = 0\ ,\tau_{3r}^0 = 0 \tag{15}$$

$$\tau_{1\theta}^0 = 0\ \ ,\tau_{2\theta}^0 = -cos\,30\ ,\tau_{3\theta}^0 = cos\,30 \tag{16}$$

$$\tau_{1z}^0 = -1\ ,\tau_{2z}^0 = -cos\,60\ ,\tau_{3z}^0 = -cos\,6 \tag{17}$$

Where z is in the axial direction and r and θ are in the radial and circumferential directions of the nanotube, respectively.

Substituting Eq. (14) into Eq. (9) and performing some algebraic manipulations, it is found that

$$\epsilon_\alpha = -\frac{1}{r^3}\left(\tau_{\alpha\theta}^0\right)^4 u_r + \frac{3}{r}\left(\tau_{\alpha z}^0\right)^2\left(\tau_{\alpha\theta}^0\right)^2\frac{\partial^2 u_r}{\partial z^2} + \left(\tau_{\alpha z}^0\right)^4\frac{\partial^3 u_r}{\partial z^3} \tag{18}$$

Inserting Eq. (18) into Eq. (13), the following equation for the microstresses is obtained

$$p_\alpha = A_0\left[-\frac{1}{r^3}\left(\tau_{\alpha\theta}^0\right)^4 u_r + \frac{3}{r}\left(\tau_{\alpha z}^0\right)^2\left(\tau_{\alpha\theta}^0\right)^2\frac{\partial^2 u_r}{\partial z^2} + \left(\tau_{\alpha z}^0\right)^4\frac{\partial^3 u_r}{\partial z^3}\right] \tag{19}$$

Similarly, substituting p_α from Eq. (19) into Eq. (11) and taking note of Eq. (14), it is found that

$$\sigma_{ij}^{(M)} = \sum_{\alpha=1}^{3}\tau_{\alpha i}^0\tau_{\alpha j}^0\sum_{\beta=1}^{3}A_{\alpha\beta}\left\{\left(\tau_{\beta r}^0\right)^2\frac{1}{r}u_r + \frac{1}{6}\eta^2\left[-\frac{1}{r^3}\left(\tau_{\beta r}^0\right)^4 u_r\right]\right\} \tag{20}$$

This equation is the relation between the macrostresses and the displacements. Setting i and j equal to θ in Eq. (20), the following equation for the normal stress $\sigma_{\theta\theta}^{(M)}$ is found

$$\sigma_{\theta\theta}^{(M)} = \sum_{\alpha=1}^{3}\left(\tau_{\alpha r}^0\right)^2\sum_{\beta=1}^{3}A_{\alpha\beta}\left\{\left(\tau_{\beta r}^0\right)^2\frac{1}{r}u_r + \frac{1}{6}\eta^2\left[-\frac{1}{r^3}\left(\tau_{\beta r}^0\right)^4 u_r\right]\right\} \tag{21}$$

If Eq. (21) is substituted into Eq. (7) and then integrated along the tube thickness, the following equation is obtained

$$N_{\theta\theta} = h\sum_{\alpha=1}^{3}\left(\tau_{\alpha r}^0\right)^2\sum_{\beta=1}^{3}A_{\alpha\beta}\left\{\left(\tau_{\beta r}^0\right)^2\frac{1}{r}u_r + \frac{1}{6}\eta^2\left[-\frac{1}{r^3}\left(\tau_{\beta r}^0\right)^4 u_r\right]\right\} \tag{22}$$

Finally, upon substituting the components of the director vectors from Eqs. (15)- (17) into Eq.(22) and the result into Eq. (12) and neglecting body forces along with taking note of Eq. (14), the following equation of motion in the radial direction for a Zigzag SWCNTs is obtained

$$-\frac{1}{r^2}u_r\left[\frac{9}{8}(a+b)\left(1-\frac{1}{8r^2}\eta^2\right)\right] = \rho\frac{\partial^2 u_r}{\partial t^2} \tag{23}$$

Eq. (23) is a second order governing equation for the RBM vibration of a nanotube in DM to within the third order of approximation. This equation can be further simplified. Since the nanotube in RBM vibration can be considered to be in the state of plane stress, from [11], it may be concluded that

$$a+b=\frac{8}{9}\frac{E}{1-\nu^2} \tag{24}$$

If Eq. (24) is substituted into Eq. (23), it is found that

$$-\frac{1}{r^2}u_r\left[\frac{E}{1-\nu^2}\left(1-\frac{1}{8r^2}\eta^2\right)\right]=\rho\frac{\partial^2 u_r}{\partial t^2} \tag{25}$$

Eq. (25) is the basic equation of motion for the RBM vibration of a Zigzag SWCNT incorporating the scale effects.

To find the frequency of RBM of the nanotube, a solution for the RBM vibration of the nanotube are assumed to be of the form

$$u_r\left(r,t\right)=\sum_{n=1}^{\infty}A_n e^{-i\,\omega^{(\eta)}t} \tag{26}$$

Where W and $\omega^{(\eta)}$ are the amplitude and frequency of the RBM vibration, respectively. Superscript η in $\omega^{(\eta)}$ indicates the natural frequency with scale effects. A_n is the amplitude of the tube vibration obtained later.

2.2 Fluid dynamics: propagation of acoustic waves

In this paper, the linearized Navier-Stokes equation for compressible flows is considered. Then, the velocity field, $\boldsymbol{v}$ is obtained by small-amplitude acoustic waves in the fluid with the following equation

$$\rho_f\frac{\partial \boldsymbol{v}}{\partial t}=-\nabla p+\mu\nabla^2\boldsymbol{v}+\left(\kappa+\frac{\eta}{3}\right)\nabla\left(\nabla\boldsymbol{v}\right) \tag{27}$$

where ρ_f is the density of the fluid, η is the shear viscosity, κ is the bulk viscosity, and p is the thermodynamic pressure.

It should be noted that bulk viscosity becomes essential where fluid compressibility is important. It is dependent to the vibrational energy of the molecules. Bulk viscosity is zero for monatomic gases with low density, but it can be large for fluids with larger molecules. It is important in describing sound attenuation and the absorption of sound energy into the fluid depends on the sound frequency like the rate of fluid compression and expansion. For an incompressible liquid the volume viscosity is superfluous, and does not appear in the equation of motion. The shear viscosity of a system measures its resistance to flow. A simple flow field can be established in a system by placing it between two plates and then pulling the plates apart in opposite directions. Such a force is called a shear force, and the rate at which the plates are pulled apart is the shear rate.

Since the vibration is purely radial, a cylindrical coordinate system located at the center of the cylinder is used. The displacement field of the elastic tube and the velocity field of the fluid, have only radial components that are functions of the distance from the origin r and time t. With this geometrical symmetry, the identity $\nabla^2 a=\nabla(\nabla.a)$ holds for a vector field $\boldsymbol{a}$, which respectively simplifies Eq. (27) to

$$\rho_f\frac{\partial \boldsymbol{v}}{\partial t}=-\nabla p+\beta\nabla^2\boldsymbol{v} \tag{28}$$

where $\beta=\kappa+\frac{4\eta}{3}$ introduced as viscosity coefficient which is zero for inviscid flow.

Now, the propagation of small-amplitude acoustic waves in the fluid surrounding for the vibrating nanotube is considered. The linearized continuity equation for a compressible fluid is given by the following equation

$$\frac{\partial\rho'}{\partial t}+\rho_f\nabla\boldsymbol{v}=0 \tag{29}$$

where $\rho'\left(r,t\right)$ represents the density fluctuation considered to be small in comparison with fluid density means $\left|\rho'\right|\ll\rho_f$. Together with the equation of state, $p=c^2\rho'$, where c is the speed of sound in the fluid, Eq. (28) can be combined with Eq. (29) to obtain the following density fluctuations equation

$$\frac{\partial^2\rho'}{\partial t^2}=c^2\nabla^2\rho'+\frac{\beta}{\rho_f}\nabla^2\frac{\partial\rho'}{\partial t} \tag{30}$$

Now, the time-periodic solution with the same vibration of the frequency of the elastic tube is sought. Then, Eq. (30) can be solved by separation of variables to yield

$$\rho'(r,t)=\rho_f\sum_{n=1}^{\infty}B_nJ_0(m_nr)e^{-i\omega_nt} \tag{31}$$

where B_n are arbitrary constants and $m_n^2=\dfrac{\omega_n^2}{c^2-\dfrac{i\beta\omega_n}{\rho_f}}$. J_0 is the Bessel function of the first kind with zero order. The corresponding velocity field can then be obtained from the continuity equation (29) as

$$v(r,t)=\sum_{n=1}^{\infty}B_n i\omega_n\frac{1}{m_n}J_1(m_nr)e^{-i\omega_nt} \tag{32}$$

3 COUPLING THE RADIAL VIBRATION OF AN ELASTIC NANOTUBE WITH THE SUUOUNDING FLUID

The vibration of the elastic nanotube is coupled with the fluid motion by matching the velocities and stresses at the boundary between the fluid and nanotube. Since small amplitude vibrations are considered, domain perturbation is used and the velocities and stresses are expanded at the boundary about the equilibrium radius of the cylinder, R, a constant, keeping only the leading-order terms. For continuity of velocity, the time derivative of the displacement field of the elastic cylinder given with Eq. (26) is computed and equated to the velocity field in the fluid obtained by Eq. (32) evaluated at $r=R$, which results in

$$\sum_{n=1}^{\infty}i\omega_nA_n=\sum_{n=1}^{\infty}B_ni\omega_n\frac{1}{m_n}J_1(m_nR) \tag{33}$$

On the other hand, the stress tensor in the solid is given by

$$\sigma_{rr}^{(M)}=\sum_{n=1}^{\infty}\frac{Eh}{r(1-\nu^2)}\left(1-\frac{1}{8r^2}\eta^2\right)A_ne^{i\omega^{(\eta)}t} \tag{34}$$

The stress tensor in the fluid is given by

$$\boldsymbol{\sigma}^f=\left[-p+k(\nabla\boldsymbol{v})\right]\boldsymbol{I}+2\eta\left(\boldsymbol{D}+\frac{\nabla\boldsymbol{v}}{3}\boldsymbol{I}\right) \tag{35}$$

where $D=\dfrac{1}{2}\left(\nabla\boldsymbol{v}+(\nabla\boldsymbol{v})^T\right)$ represents the rate of strain tensor. The only nonzero component of the stress tensor $\boldsymbol{\sigma}$ is

$$\sigma_{rr}^f=-c^2\rho_f\sum_{n=1}^{\infty}B_nJ_0(m_nr)e^{-i\omega_nt}+\sum_{n=1}^{\infty}\left(k+\frac{2\eta}{3}\right)\left[i\omega_n\sum_{n=1}^{\infty}B_nJ_0(m_nr)e^{-i\omega_nt}\right]+2\eta\left[\sum_{n=1}^{\infty}B_ni\omega_nJ_1'(m_nr)e^{-i\omega_nt}\right] \tag{36}$$

Simplification on Eq. (36) yields

$$\sigma_{rr}^f=\sum_{n=1}^{\infty}B_n\left\{-c^2\rho_fJ_0(m_nr)+i\omega_n\left(k+\frac{2\eta}{3}\right)J_0(m_nr)-2\eta i\omega_n\left[J_0(m_nr)-J_2(m_nr)\right]\right\}e^{-i\omega_nt} \tag{37}$$

where the equation of state and the continuity equation have been used. Evaluating and matching the stresses in the solid and fluid given respectively with Eq. (34) and Eq. (37) at *r=R* via relation between stresses for thin-walled cylinders under pressure, leads to

$$\frac{1}{R}\sum_{n=1}^{\infty}\frac{Eh}{R(1-\nu^2)}\left(1-\frac{1}{8R^2}\eta^2\right)A_ne^{i\omega^{(\eta)}t}=\frac{1}{h}\sum_{n=1}^{\infty}B_n\left\{-c^2\rho_fJ_1(m_nR)+i\omega_n\left(k+\frac{2\eta}{3}\right)J_1(m_nR)+\eta i\omega_nm_n\left[J_0(m_nR)-J_2(m_nR)\right]\right\} \tag{38}$$

The two boundary conditions in Eqs. (33) and (38) can be rearranged as follow

$$\begin{bmatrix} -i\omega_n & i\omega_n \frac{1}{m_n} J_1(m_n R) \\ -\frac{Eh}{R^2(1-\nu^2)}\left(1-\frac{1}{8R^2}\eta^2\right) & \frac{1}{h}\left\{-c^2\rho_f J_0(m_n R)+i\omega_n\left(k+\frac{2\eta}{3}\right)J_0(m_n R)-\eta i\omega_n\left[J_0(m_n R)-J_2(m_n R)\right]\right\} \end{bmatrix} \begin{bmatrix} A_n \\ B_n \end{bmatrix} = 0 \tag{39}$$

For non-trivial solution to the system of equations in Eq. (39), it is required that the determinant of the matrix representing this system must be zero, which leads to the eigenvalue equation for the natural frequencies ω

$$-c^2\rho_f J_0(m_n R)+i\omega_n\left(k+\frac{2\eta}{3}\right)J_0(m_n R)-\eta i\omega_n\left[J_0(m_n R)-J_2(m_n R)\right]-hi\omega_n\frac{1}{m_n}J_1(m_n R)\times\frac{Eh}{R^2(1-\nu^2)}\left(1-\frac{1}{8R^2}\eta^2\right)=0 \tag{40}$$

It is notable that Eq. (40) is a transcendental equation and should be solved numerically. With solving Eq. (40), a complex frequency is obtained as $\omega=\omega_r+\omega_i i$, where ω_r and ω_i are, respectively, the real and imaginary parts of the frequency. The imaginary part of complex conjugate root can be considered as a criterion for severity of damping. When this coefficient increases, the vibration will damp in lesser time. It should be added that this parameter has no influence on the main (real) frequency.

Here, only the results for the fundamental mode (n = 1) is calculated, since it is mainly the mode detected in experimental measurements. Although, higher order modes can be obtained by finding other roots of the same equation. For an inviscid flow ($\eta=\kappa=0$), the eigenvalue condition (40) for ω reduces to

$$-c^2\rho_f J_0(m_n R)-hi\omega_n\frac{1}{m_n}J_1(m_n R)\times\frac{Eh}{R^2(1-\nu^2)}\left(1-\frac{1}{8R^2}\eta^2\right)=0 \tag{41}$$

The case $\rho_f=0$ corresponds to an elastic cylinder radially vibrating in a vacuum [13] where the eigenvalue condition further simplifies to

$$J_1(k_n R)=0 \tag{42}$$

It should be noted that the attenuation in oscillation is not due to viscous dissipation in the fluid since an inviscid medium is considered in Eq. (41). Instead, the attenuation comes from the propagation of energy into the surrounding medium away from the vibrating tube. Compressibility in the fluid provides a mechanism for energy to propagate away from the vibrating tube through acoustic waves. When the shear and bulk viscosities of fluid are taken into account, Eq. (41) gives a slightly reduced. For inviscid flow, all damping is due to the propagation of acoustic waves away from the source. It should also be pointed out that when the breathing mode of an elastic tube surrounded by another elastic medium is considered, the eigenvalue conditions can be alternatively obtained by modifying the constitutive relation to include the viscous contribution from the fluid. For the case of vacuum surrounding the vibrating cylinder, the frequencies determined from Eq. (42) are real because there is no damping outside the cylinder. When the vacuum is replaced by an inviscid fluid medium, the frequencies determined from the roots of Eq. (41) become complex, which implies that the free oscillation of the elastic cylinder in a fluid takes the form of a sinusoid attenuating exponentially.

4 RESULT AND DISCUSSION

To show the validity and accuracy of the present analysis, numerical results are calculated to compare with those available in the literature. Table 2 compares the RBM frequencies of the different SWCNTs vibrating in vacuum obtained from different methods. Reasonable agreement between the present solutions and those given in the other literature is achieved. Experimentally, the RBMs frequency is related to ω via $f = w/2\pi C$ where $C=2.99792458\times10^{10}cm/s$ is the velocity of light in the vacuum. This relation is used in Tables 1 below to report the frequencies in cm^{-1}. Throughout this paper, the material properties of SWCNT are taken to be: Young's modulus $E=1.059TPa$, mass density $\rho=2270kg/m^3$ and Poisson's ratio $\nu=0.2$ [13]. In the DM model, the scale parameter used is the carbon-carbon bond length $\eta=0.1421nm$ and equilibrium interlayer spacing between two adjacent tubes is considered to be equal to 0.34 *nm* [16].

Table 2

Frequencies of RBMs (cm^{-1}) for various SWCNTs with different methods

Tube chirality	Tube diameter	RBM [13]	Experimental result [33]	Present method	Percent of differences between present method and experimental result
(9,0)	0.7047	317.4	317.2	317.2	0
(10,0)	0.7830	286.2	285.4	285.6	0.0007
(6,6)	0.8138	275.1	274.6	274.7	0.0011
(11,0)	0.8613	260.5	259.5	259.8	0.0012
(12,0)	0.9397	239.1	237.8	238.1	0.0013
(7,7)	0.9494	236.4	235.4	235.7	0.0013
(13,0)	1.0180	220.9	219.5	219.9	0.0018
(8,8)	1.0850	207.2	206.0	206.4	0.0019
(14,0)	1.0963	205.2	203.9	204.3	0.0029
(15,0)	1.1746	191.7	190.3	190.7	0.0021
(9,9)	1.2206	184.3	183.1	183.5	0.0022
(16,0)	1.2529	179.8	178.4	178.8	0.0022
(17,0)	1.3312	169.3	167.9	168.3	0.0024
(10,10)	1.3563	166.0	164.8	165.1	0.0018
(18,0)	1.4095	159.9	158.6	158.9	0.0019
(19,0)	1.4878	151.5	150.2	150.6	0.0027
(11,11)	1.4919	151.0	149.8	150.1	0.0020
(20,0)	1.5661	144.0	142.7	143	0.0021

The calculations for frequency in radial vibration of SWCNTs vibrating in fluid are also given in graphical form in Figs. 3- 5. To study the effects of different physical parameters on vibration frequency, the breathing mode of a single nanotube in water was measured. Fig. 3 shows the frequency variations versus fluid density for different mode number for Zigzag (16, 0). As can be seen from this figure, in contrast to a systems vibrating in vacuum, the frequencies are a function of fluid density so that as the density increases, the frequency decreases. As fluid density increases more, the more pronounced reduction between the frequencies become. It can also be seen that as the mode number increases, the frequency increases too. It can also be seen that reduction of frequency with fluid density is more sensitive in higher mode numbers.

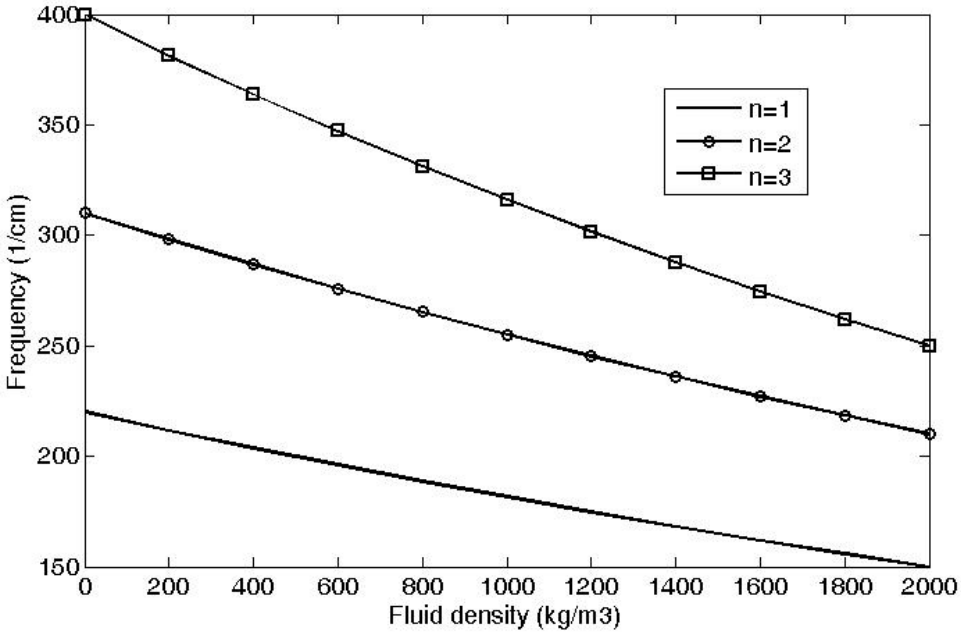

Fig. 3
Frequency versus fluid density for different mode numbers.

Fig. 4 illustrates the frequency variations against the tube diameter in different viscosity coefficients. It can be observed that with the increase of the tube diameter, the frequencies of SWCNTs decrease. The decreasing rate for the frequency is more apparent for lower tube diameter. As is expected, frequency is lesser in the higher viscosity coefficient. It is due to the existence of viscose fluid around the tube which has damping effect for the tube. As said before the attenuation of fluid energy comes from the propagation of energy into the surrounding medium away from the vibrating tube. When the shear and bulk viscosities of fluid are taken into account, result may give a slightly reduced. For inviscid flow, all damping is due to the propagation of acoustic waves away from the source. It is also seen that as the tube diameter increases more, the frequencies tend to approach the single value. This effect is more pronounced for tubes with higher viscosity coefficient around it.

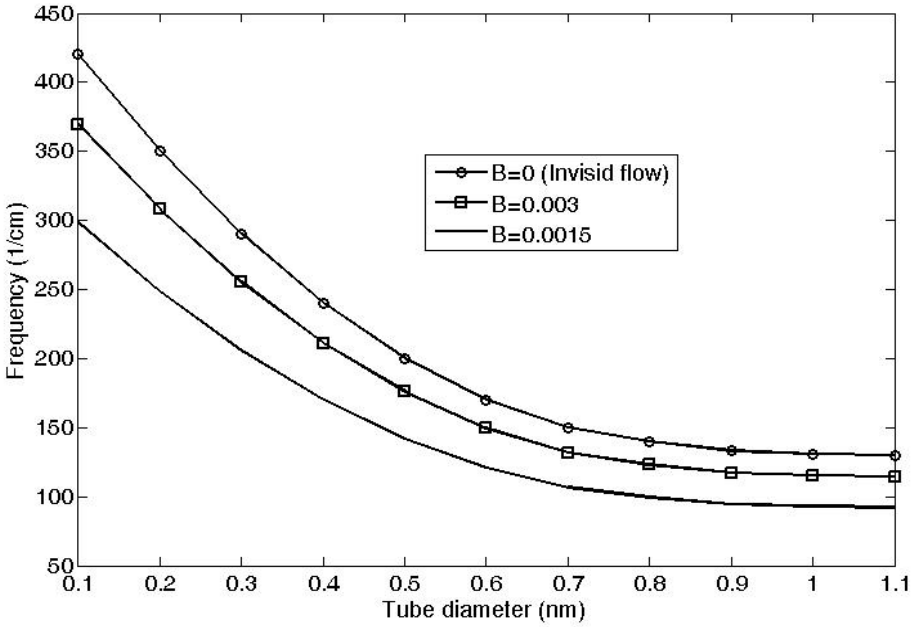

Fig. 4
Frequency versus fluid density for different mode numbers.

Variations of frequency versus shear viscosity have been plotted in Fig. 5 for Zigzag and Armchair tubes. As seen from this figure, as the shear viscosity increases, the frequencies decreases. This reduction is more apparent in higher shear viscosity. It may be because of the increased viscous dissipation. It is also seen that the vibration frequency of Zigzag nanotubes is fewer more than the Armchair one or Armchair nanotubes is stiffer than the Zigzag one. It may be because this reason that microstructural interaction between viscosity and scale effect is more significant in Zigzag one.

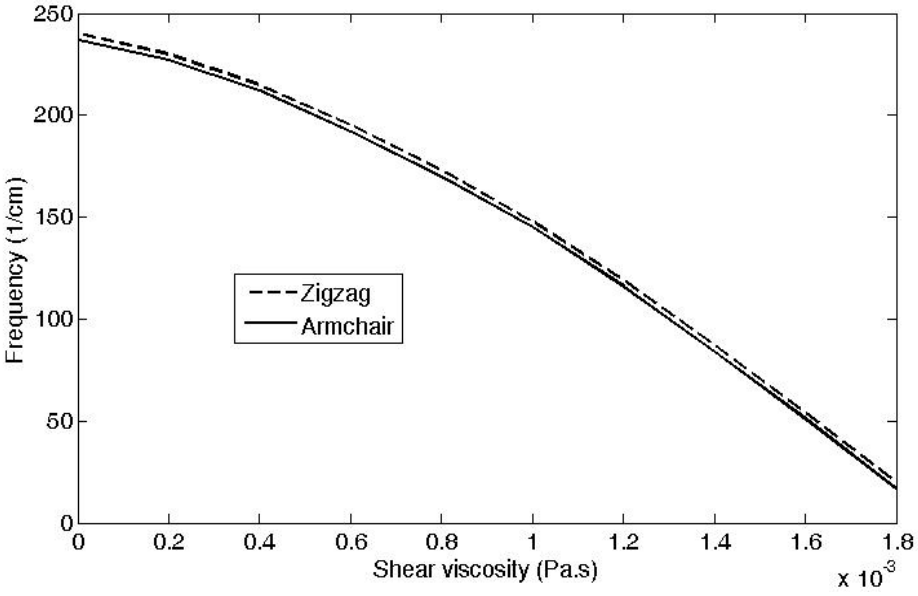

Fig 5
Frequency versus shear viscosity for Zigzag and Armchair nanotubes.

5 CONCLUSIONS

In this paper, the frequencies of a radially oscillating elastic nanotube in simple and complex fluid media have been studied. The equations of motion for solid tube are derived based DM considering reaction between fluid and nanotube in the boundary using Navier-Stoke's equation. First, a nanotube vibrations in vacuum is considered and then the Newtonian fluid media around the tube taking into account with considering both shear and viscosities, and demonstrated that the fluid compressibility plays a significant role in the radial vibration of nanotubes. Due to the simplicity of the tube geometry considered in this work, the eigenvalue equation for the breathing mode in the fluid medium is exact and analytical while is solved numerically. To show the accuracy and ability of this method, the generated results obtained have been compared with available results and reasonable agreement has been achieved. The main results specifically obtained in this paper are as follows.

1- Due to the coupling and interaction between the fluid and structure, frequency of the tube vibrating in fluid is dependent to the fluid properties too. Because of fluid compressibility, the frequency is attenuated and obtained as complex form which in real part is the main frequency and the imaginary part represents the damping severity.
2- The frequency of the tube has inverse proportion with fluid density. As the fluid density increases, the tube frequency decreases. This reduction is more significant for higher mode numbers.
3- As the viscosity coefficient increases, the frequency decreases. Similar behavior is seen with tube diameter.
4- The shear viscosity has decreasing effect on tube frequency. This reduction is more significant for higher values of shear viscosity. For the same shear viscosities, the frequency of Zigzag nanotube is slightly higher than the Armchair one.

REFERENCES

[1] A Fatahi-Vajari, Z Azimzadeh, Natural Frequency of Rotating Single-Walled Carbon Nanotubes with Considering Gyroscopic Effect, Journal of Solid Mechanics, 12(1), 136-147 (2020).
[2] S. S.Verbridge, L. M. Bellan, J. M. Parpia, and H. G. Craighead, Optically driven resonance of nanoscale flexural oscillators in liquid, Nano Letters, 6, 2109–2114 (2006).
[3] A. Casto, F.M. Bellussi, M. Diego, N.D. Fatti, F. Banfi, P.Maioli, M.Fasano, Water filling in carbon nanotubes with different wettability and implications on nanotube/water heat transfer via atomistic simulations, International Journal of Heat and Mass Transfer, 205, 123868 (2023).
[4] B. Stephanidis, S. Adichtchev, P. Gouet, A. McPherson, and A. Mermet, Elastic properties of viruses, Biophysical Journal, 93(4), 1354–1359 (2007).
[5] M. M. Seyyed Fakhrabadi, A. Rastgoo, M. Taghi Ahmadian, Application of electrostatically actuated carbon nanotubes in nanofluidic and bio-nanofluidic sensors and actuators, Measurement, 73, 127-136 (2015).
[6] J. L. Arlett, E. B. Myers, and M. L. Roukes, Comparative advantages of mechanical biosensors, Nature Nanotechnology, 6, 203–215 (2011).
[7] B. Li, Y. Wei, F. Meng, P. Ou, Y. Chen, L. Che, C. Chen, J. Song, Atomistic simulations of vibration and damping in three-dimensional graphene honeycomb nanomechanical resonators, Superlattices and Microstructures, 139, 106420 (2020).
[8] X. Yi, B. Li, Z. Wang, Vibration Analysis of Fluid Conveying Carbon Nanotubes Based on Nonlocal Timoshenko Beam Theory by Spectral Element Method, Nanomaterials, 9(12), 1780 (2019).
[9] V. Galstyan, O. S. Pak, and H. A. Stone, A note on the breathing mode of an elastic sphere in Newtonian and complex Fluids, 27, 032001.1-032001.13 (2015).
[10] P. V. Ruijgrok, P. Zijlstra, A. L. Tchebotareva, and M. Orrit, Damping of acoustic vibrations of single gold nanoparticles optically trapped in water, Nano Letters, 12, 1063–1069 (2012).
[11] A. Fatahi-Vajari, A. Imam, Torsional vibration of single-walled carbon nanotubes using doublet mechanics, ZAMP, 67, 81 (2016).
[12] A. Fatahi-Vajari, A new method for determination of natural frequency in bending vibration mode of single-walled carbon nanotubes, Journal of Simulation and Analysis of Novel Technologies in Mechanical Engineering, 13(1), 5-18 (2021).
[13] A. Fatahi-Vajari, A. Imam, Analysis of radial breathing mode vibration of single-walled carbon nanotubes via doublet mechanics, ZAMM, 96(9), 1020-1032 (2016).
[14] M.R. Ebrahimian, A. Imam, and M. Najafi, Doublet mechanical analysis of bending of Euler-Bernoulli and Timoshenko nanobeams, ZAMM, 98(9), 1642-1665 (2018).
[15] M.R. Ebrahimian, A. Imam, and M. Najafi, The effect of chirality on the torsion of nanotubes embedded in an elastic medium using doublet mechanics, Indian Journal of Physics, 94(1), 31-45, (2020).
[16] M.R. Ebrahimian, Z. Azimzadeh, A. Fatahi-Vajari, M. Shariati, Nonlinear coupled torsional-radial vibration of single-walled carbon nanotubes using numerical methods, Journal of Computational Applied Mechanics 52(4), 642-663 (2021).
[17] M.R. Ebrahimian, D. Shokri, B. Tabibian, M.R. Allahverdlou, M.S. Atlasbaf, Analytical Response of Nonlinear Buckling of Composite Plates Reinforced with Graphene Nanosheets, Transactions on Machine Intelligence, 6(2), 76-88 (2023).

[18] D. Chakraborty, E. van Leeuwen, M. Pelton, and J. E. Sader, Vibration of nanoparticles in viscous fluids, Journal of Physical Chemistry C, 117, 8536–8544 (2013).
[19] D. Xiang , J. Wu , J. Rottler, R. Gordon, Threshold for Terahertz Resonance of Nanoparticles in Water, Nano Letters, 16(6), 3638-3641 (2016).
[20] J. Lermé , J. Margueritat , A. Crut, Vibrations of Dimers of Mechanically Coupled Nanostructures: Analytical and Numerical Modeling, Journal of Physical Chemistry C, 125(15), 8339–8348 (2021).
[21] M. A. Dheyab, A. A. Aziz, P. M. Khaniabadi, M. S. Jameel, N. Oladzadabbasabadi, S. A. Mohammed, R. S. Abdullah, B. Mehrdel, Monodisperse Gold Nanoparticles: A Review on Synthesis and Their Application in Modern Medicine, International Journal of Molecular Sciences, 23(13), 7400 (2022)
[22] M. Pelton, D. Chakraborty, E. Malachosky, P. Guyot-Sionnest, and J. E. Sader, Viscoelastic flows in simple liquids generated by vibrating nanostructures, Physical Review Letters, 111, 244502 (2013).
[23] Y. Yan, W.Q. Wang, L.X. Zhang and X.Q. He, Dynamical behaviors of fluid-conveyed multi-walled carbon nanotubes, Applied Mathematical Modelling, 33, 1430-1440 (2009).
[24] T. Natsuki, Q. Q. Ni and M. Endo, Wave propagation in single- and double-walled carbon nanotubes filled with fluids, Journal of Applied Physics, 101, 034319.1-034319.5 (2007).
[25] K. Dong, X. Wang and G. G. Sheng, Wave dispersion characteristics in fluid-filled carbon nanotubes embedded in an elastic medium, Modelling and Simulation in Materials Science and Engineering, 15(5), 427-439 (2007).
[26] A.H. Ghobanpour Arani, A Rastgoo, A. Ghorbanpour Arani, M. S. Zarei, Nonlocal Vibration of Y-SWCNT Conveying Fluid Considering a General Nonlocal Elastic Medium, Journal of Solid Mechanics, 2(8), 232-246 (2016).
[27] J. Rexy, R. Selvamani, R. Kumar, M. Mahaveersree Jayan, Nonlocal Dispersion Analysis of a Fluid–Conveying Thermo Elastic Armchair Single Walled Carbon Nanotube Under Moving Harmonic Excitation, Journal of Solid Mechanics, 12(1), 189-203 (2020).
[28] Z. Azimzadeh, A. Fatahi-Vajari, Coupled Axial-Radial Vibration of Single-Walled Carbon Nanotubes Via Doublet Mechanics, Journal of Solid Mechanics, 11(2), 323-340 (2019).
[29] A. Fatahi-Vajari, Z. Azimzadeh, Analysis of Coupled Nonlinear Radial-Axial Vibration of Single-Walled Carbon Nanotubes Using Numerical Methods, Journal of Solid Mechanics, 12(4), 862-882 (2020).
[30] A. Kanani, M. Mahnama, E. Ghavaminezhad, Investigation of vibration of carbon nanotube and quality factor with confined and submerged fluid under hammer impact Test: A molecular dynamics study, Journal of Molecular Liquids, 394, 123633 (2024).
[31] X. Yi, B. Li, Z. Wang, Vibration Analysis of Fluid Conveying Carbon Nanotubes Based on Nonlocal Timoshenko Beam Theory by Spectral Element Method, Nanomaterials, 9(12), 1780 (2019).
[32] A. Fatahi-Vajari, A new method for evaluating the natural frequency in radial breathing like mode vibration of double-walled carbon nanotubes, ZAMM, 98(2), 255-269 (2018).
[33] S. Basirjafari, S.E. Khadem, R. Malekfar, Radial breathing mode frequencies of carbon nanotubes for determination of their diameters, Current Applied Physics 13, 599–609 (2013).
[34] A. Fatahi-Vajari, A. Imam, Axial vibration of single-walled carbon nanotubes using doublet mechanics, Indian Journal of Physics, 90(4), 447–455 (2016).
[35] M. Ferrari, V.T. Granik, A. Imam, J.C. Nadeau, Advances in Doublet Mechanics, Springer (1997)
[36] A. Fatahi-Vajari, A. Imam, Lateral Vibrations of Single-Layered Graphene Sheets Using Doublet Mechanics, Journal of Solid Mechanics, 8(4), 875-894 (2016).
[37] M. Hussain, A.O.M. Alzahrani, M.A. Khadimallah, S. Alghamdi, A. Fatahi-Vajari, A. Tounsi, Based on Euler beam theory to evaluate the GHz frequencies versus length-to-radius ratios: Continuum model, Advances in Concrete Construction, 14(4), 291-298 (2022).